Direct measurement of the Aharonov-Casher phase and tensor Stark polarizability using a calcium atomic polarization interferometer

Shinya Yanagimachi, Masaki Kajiro, Mamoru Machiya, and Atsuo Morinaga
Department of Physics, Faculty of Science and Technology, Tokyo University of Science, 2641 Yamazaki, Noda-shi, Chiba 278-8510, Japan

(Received 15 November 2001; published 14 March 2002)

An atomic polarizing white-color interferometer composed of the wave packets in the $m=+1$ and $m=-1$ states of the excited $^3P_1$ state of Ca, has been developed using a thermal atomic beam excited by a pair of two resonant lights at two separate zones under a homogeneous magnetic field. The interferometer generated the Ramsey fringes as a detuning of the rf frequency between two resonant lights from the Zeeman-frequency shift, while it generates white-color interference fringes as a detuning of laser frequency. The interferometer was used for the direct and short-time measurement of the Aharonov-Casher phase by removing the main part of dc Stark phase shift and without the influence of the frequency fluctuation of a laser. The measured dependence of the Aharonov-Casher phase on the electric field agreed with the predicted one within a relative uncertainty of 2.9%. The tensor polarizability in the $^3P_1$ state was determined to be $\alpha_2=2.623\pm0.015$ kHz/(kV/cm)^2 from the frequency shift between the $m=+1$ and $m=-1$ states.

DOI: 10.1103/PhysRevA.65.042104 PACS number(s): 03.65.Ta, 03.75.Dg, 32.60.+i, 42.50.Vk

I. INTRODUCTION

In 1984, Aharonov and Casher predicted that a neutral particle with a magnetic moment $\boldsymbol{\mu}$, traveling a closed path around a line charge, experiences a phase shift given by

$$\Delta\psi_{AC}=\frac{1}{\hbar c^2}\oint \boldsymbol{\mu}\times\mathbf{E}dr, \tag{1}$$

where $\mathbf{E}$ is the electric field due to the line charge [1]. This Aharonov-Casher (AC) effect is analogous to the Aharonov-Bhom effect [2], in which an electromagnetic vector potential shift in the phase of the de Broglie wave of charged particles, even if classical forces are absent.

The AC effect was first tested by Cimmino *et al.* using a neutron interferometer [3]. The experiment over a period of more than three months confirmed the existence of the AC effect although the observed phase was nearly two standard deviations above the theoretical value. After that, to improve the uncertainty, Sangster and co-workers used the atomic systems of TlF and rf Ramsey resonance method [4,5]. Because the atomic system produced a high-flux beam and the difference of the phase between the up and the down nuclear magnetic moment could be measured as the resonance-frequency shift precisely. They succeeded to reduce the uncertainty remarkably, and for the first time demonstrated that the AC effect is proportional to the strength of electric field and independent of the particle velocity. The magnetic moment of atoms is about two thousand times larger than that of a neutron or nuclear. Therefore, Gorlits *et al.* measured the AC phase using the ground state of Rb atom prepared in the $F=3$ state with $\Delta m=2$ spin coherence [6]. They detected the resonance shift of the Ramsey fringes in a nonlinear Faraday rotation and their result was in good agreement with the predictions within 1.4%. The AC effect of the atom was also measured by Zeiske *et al.* using a Ca optical Ramsey resonance with a high accuracy of 10 Hz [7]. As the dc Stark phase shift of the Ca atom was ten-thousands times larger than the AC phase, an integration time of as much as 8000 s per datum for the measurement of the optical frequency was performed to verify the AC shift within 2.2%.

Thus, up to now it seems to us that the Aharonov-Casher effect has been verified completely. However, in the above three experiments, the AC phase was converted from the resonance frequency using the knowledge of the velocity of the atom, although the AC phase is nondispersive. In order to measure the nondispersive phase, a white-color interferometer is preferable. The huge dc Stark phase observed in the Ca-atom interferometer could be canceled out, if we compare the phase between the wave packets of the $m=+1$ and $m=-1$ states by using a polarizing interferometer. Therefore, if the atomic polarizing white-color interferometer could be developed, a direct and a comparatively short-time measurement of the AC phase will be possible.

Previously, we developed a symmetric Ramsey-Bordé atom interferometer comprised of copropagating traveling laser beams [8,9]. This interferometer works as a white colored one with a phase that does not depend on the frequency fluctuation of the excited laser. Usual Ramsey-Bordé atom interferometers use the wave packets in the ground state and the metastable excited state as its arms [10]. Both states have different polarizabilities, therefore, the interference fringes are washed out by the dispersive dc Stark effect [11].

On the other hand, recently we developed a polarizing interferometer with wave packets of $m=+1$ and $m=-1$ in excited states in their arms. This is done by exciting the atomic beam using two resonance frequencies, which were resonant to the $m=1$ state or $m=-1$ state from the ground state, by turns [12]. Succeedingly, by exciting atoms with two resonance frequencies at the same time, we could produce an atomic polarizing interferometer, in which two wave packets of the $m=+1$ and $m=-1$ state propagating on the same path interfere. This interferometer still has the performance of the white color interferometer. Therefore, using

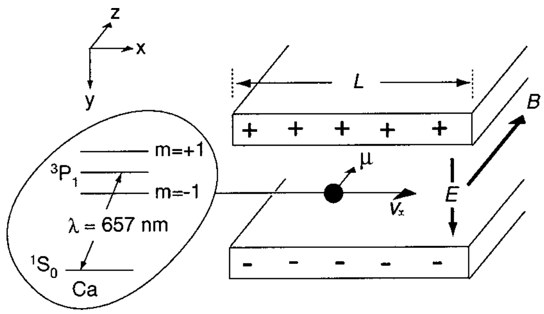

FIG. 1. Field configuration for the Aharonov-Casher effect and a partial energy diagram of Ca. The Ca atom with a velocity of v_x travels perpendicular to both an electric field E along the y axis and a magnetic field B along the z axis. L is a length of the electric field.

this interferometer, the AC phase could be measured directly without the knowledge of atomic velocity and the dc Stark phase shift.

In the present paper, we describe the performances of the atomic polarizing white color interferometer and present the results of the direct AC phase measurement together with the measurement of the tensor polarizability of $^3P_1$ state of calcium.

II. PHASE SHIFT OF Ca ATOM UNDER THE ELECTRIC AND MAGNETIC FIELDS

In order to observe the AC effect in an atomic system, Sangster and co-workers demonstrated an intelligent configuration, where the two coherently split beams with different magnetic moments (μ_a and μ_b) travel through the same path in a uniform electric field instead of a line charge [4,5]. If the beam travels a distance L along the x axis and E lies on the y axis, the AC phase shift between the two arms of the interferometer is given by

$$\Delta\psi_{AC} = -\frac{EL}{\hbar c^2}([\mu_z]_a - [\mu_z]_b), \tag{2}$$

where $[\mu_z]_a$ and $[\mu_z]_b$ are z components of the magnetic moment. Therefore, if $[\mu_z]_a \neq [\mu_z]_b$, the recombination of the two beams generates the interference fringes with the AC phase shift. However, if we use this configuration of a neutral atom having a polarizability, the dc Stark phase shift must be taken into account [13].

Let us consider the phase shift of a Ca atom in the $^1S_0$ ground state or $^3P_1$ excited state, which moves in the x direction in the homogeneous electric and magnetic fields, as shown in Fig. 1. The excited state $^3P_1$ has a long lifetime of 0.57 ms [14], and the intercombination line between the states of $^1S_0$ and $^3P_1$ is 657 nm. Under the homogeneous magnetic field B, which is applied along z axis, the $^3P_1$ state is split into $m=+1,0,-1$ a magnetic substates. The excited $^3P_1$ state has a scalar and tensor polarizability of $\alpha_{0,e}$ and $\alpha_{2,e}$ and a magnetic dipole moment μ. The ground $^1S_0$ state has only a scalar polarizability of $\alpha_{0,g}$.

The interaction between a calcium atom and the external static fields is given by the following perturbation Hamiltonian:

$$H' = m_z \mu B - \tfrac{1}{2}\{\alpha_0 + \alpha_2(3m_y^2 - 2)\}E^2. \tag{3}$$

The internal energy of the $|^3P_1, m\rangle$ state is shifted by

$$\Delta\varepsilon = -\tfrac{1}{2}(\alpha_{0,e} + \alpha_{2,e})E^2, \quad m=0,$$

$$\Delta\varepsilon = -\tfrac{1}{2}\alpha_{0,e}E^2 + \tfrac{1}{4}\alpha_{2,e}E^2 + m\sqrt{(\mu B)^2 + \tfrac{9}{16}(\alpha_{2,e}E^2)^2}, \quad m=\pm 1. \tag{4}$$

Using the Eikonal approximation, when a wave packet in the $|^3P_1, m\rangle$ state travels in the fields for a distance L, the phase is shifted by

$$\Delta\psi = -\frac{1}{2}(\alpha_{0,e} + \alpha_{2,e})E^2 \frac{L}{\hbar v_x}, \quad m=0,$$

$$\Delta\psi = \left\{ -\tfrac{1}{2}\alpha_{0,e}E^2 + \tfrac{1}{4}\alpha_{2,e}E^2 + m\left(|\mu B| + \frac{9}{32}\frac{\alpha_{2,e}^2 E^4}{|\mu B|} \right) \right\} \frac{L}{\hbar v_x}, \quad m=\pm 1, \tag{5}$$

where v_x is the velocity of the atom in the x direction. The second term is an approximation value under the condition that $|\alpha_{2,e}E^2|$ is smaller than $|\mu B|$. On the other hand, the phase of a wave packet in the $|^1S_0, 0\rangle$ state is shifted by

$$\Delta\psi = -\frac{1}{2}\alpha_{0,g}E^2 \frac{L}{\hbar v_x}. \tag{6}$$

Therefore, by taking the AC phase shift into acount, the total phase difference between two beams in these states can be derived from Eqs. (2), (5), and (6).

For example, if we take the $|^3P_1, +1\rangle$ state and the $|^1S_0, 0\rangle$ state as two beams, then the phase difference is

$$\Delta\psi = \left\{ -\tfrac{1}{2}(\alpha_{0,e} - \alpha_{0,g})E^2 + \tfrac{1}{4}\alpha_{2,e}E^2 + \left(|\mu B| + \frac{9}{32}\frac{\alpha_{2,e}^2 E^4}{|\mu B|} \right) \right\} \frac{L}{\hbar v_x} - \frac{\mu E L}{\hbar c^2}. \tag{7}$$

The first term is the quadratic Stark phase due to the difference between the polarizabilities of the ground and excited states. Zeiske *et al.* used the atom interferometer in the optical Ramsey geometry that produced this phase shift. The Stark phase was roughly ten-thousand times larger than the AC phase [7]. Therefore, they suppressed the influence of the quadratic Stark effect by inverting the electric field at a constant field strength.

On the other hand, if we use the $|^3P_1,+1\rangle$ state and the $|^3P_1,-1\rangle$ state, then the phase difference is

$$\Delta\psi=2\left(|\mu B|+\frac{9}{32}\frac{\alpha_{2,e}^2E^4}{|\mu B|}\right)\frac{L}{\hbar v_x}-2\frac{\mu EL}{\hbar c^2}. \tag{8}$$

In this case, the quadratic Stark phase shift disappears. The first term is the dynamical Zeeman phase between two beams, but it can be canceled out in the case of our atom interferometer that is described in the following section. The last term is the AC phase. The second term is the tensor Stark split for the $m=\pm1$ state, which is proportional to the fourth power of the electric field and inversely proportional to μB. Therefore, it should be noted that there is still a small phase shift depending on the electric field besides the AC effect.

III. ATOMIC POLARIZING WHITE-COLOR INTERFEROMETER

A. Principle

Usual Ramsey-Bordé atom ineterferometers use two wave packets in the two different states, one of which is the ground state and the other is the long-lived excited state. Up to now, there is no atom interferometer between the two excited states. However, we could demonstrate a Ramsey-Bordé atom interferomter having two arms with different Zeeman sublevels by utilizing the excitation of a pair of two opposite circularly polarized laser beams, which are tuned to each resonance frequency in a sequence of $\sigma^+-\sigma^+-\sigma^--\sigma^-$ [11]. In this configuration, one wave packet in the $m=+1$ state runs during the first and the second excitation zones and the other wave packet in the $m=-1$ state runs during the third and the fourth zones. Consequently, the dc Stark phase shift due to inhomogeneity of the electric field still remains.

Figure 2 shows the configuration of our new interferometer. The atomic beam in the ground state moves in the x direction and interacts with the two laser beams, which propagate along the z direction. A homogeneous magnetic field B is also applied in the z direction in order to split the magnetic sublevels. Each laser beam has two components, one of which is circularly σ^+ polarized and shifted in frequency $+\Delta\nu$ from the carrier frequency of the laser, ν_L. The other is circularly σ^- polarized and shifted in frequency $-\Delta\nu$ from ν_L. The frequency shift $\Delta\nu$ is produced by the electro-optic modulator driven by a synthesizer. $\Delta\nu$ is close to the Zeeman frequency shift of $\Delta\nu_B=\mu B/h$.

In the first excitation zone, an atom interacts with two components of the laser beam, and a part of the wave packet is excited to the $^3P_1$, $m=+1$ state, and another part is excited to the $^3P_1$, $m=-1$ state with almost the same recoil velocity. After both the wave packets move along the same path for beam spacing D in the homogeneous magnetic

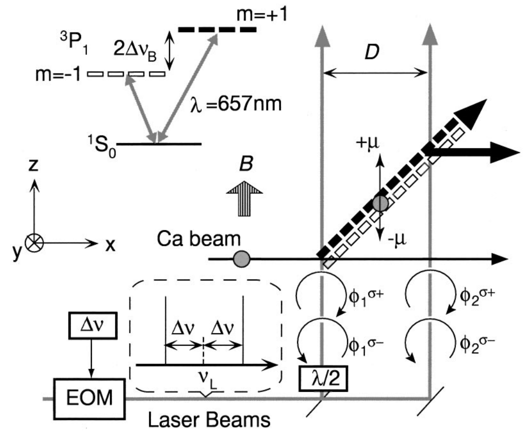

FIG. 2. Scheme of the Ca atomic polarizing white-color interferometer under a magnetic field B. A calcium atomic beam is excited at two separate zones by a pair of σ^+- and σ^--polarized laser beams. The solid line, ground state; broken black line, excited $m=+1$ state; broken white line, excited $m=-1$ state; gray line, laser beams; $\phi_i^{\sigma+}$, phase of the ith σ^+-polarized laser beam; $\phi_i^{\sigma-}$, phase of the ith σ^--polarized laser beam; EOM, electro-optic modulator driven at a frequency of $\Delta\nu$; λ/2, half-wave plate; the frequency and polarization of laser beams are shown in the figure.

fields, they interact with the second laser beam with the same components as the first laser beam. In the second excitation zone, the wave packet in the $^3P_1$, $m=+1$ state is changed to $m=-1$ state through ground state, by stimulated emission and absorption of two photons and vice versa. The new wave packet of $m=+1(-1)$ combines with the wave packet of $m=+1(-1)$ and interferes. Both the interference fringes have the same phase, so that the fringes generate cooperatively. On this point, the mechanism differ from the two-photon stimulated Ramn process [15].

The phase difference of these wave packets can be calculated based on the phase shift arising from the interaction of the atom with light and the phase shift due to the free evolution of atoms between interactions [12]. Under a homogeneous magnetic field, the total phase shift $\Delta\psi$ is given by

$$\Delta\psi=(\pi-\phi_1^{\sigma+}+\phi_1^{\sigma-}+\phi_2^{\sigma+}-\phi_2^{\sigma-})+2\pi(\Delta\nu-\Delta\nu_B)\frac{2D}{v_x}, \tag{9}$$

where v_x is the initial velocity of atoms in the x direction. ϕ_i^{σ} is the phase of the laser beam at interaction zone i. The first term is the optical phase difference between laser beams. The second term means that the dynamical phase shift between both wave packets due to a magnetic field [which is discussed in Eq. (8)] is canceled out by the frequency difference between two laser beams. Therefore, we can observe the Ramsey fringe as detuning the $\Delta\nu-\Delta\nu_B$. The period of Ramsey fringes is given by $v_x/2D$, which is half of the usual Ramsey fringes. On the other hand, the phase does not change as tuning the carrier frequency of the laser, as usual symmetrical atom interferometer [8]. Generally, this kind of atom interferometer can be constructed between any two long-lived excited states, if the energy difference is in the region of the microwave frequency [16].

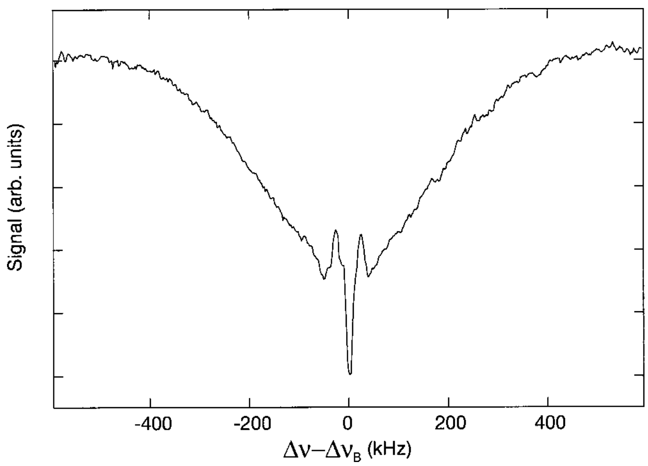

FIG. 3. Fluorescence signal as a function of $\Delta\nu-\Delta\nu_B$ when a spacing of the laser beams is 8.1 mm. The scanning rate of the $\Delta\nu-\Delta\nu_B$ was 1.2 MHz per 10 s.

B. Experimental result

The experimental setup was almost the same as described in Ref. [12]. A thermal calcium atomic beam with the most probable velocity of 810 m/s was generated from the oven. The laser light with a wavelength of 657 nm for exciting the $^1S_0$ to the $^3P_1$ state was generated from a high-resolution diode laser spectrometer. The output laser beam with a frequency of ν_L was introduced into a resonant-type electro-optic modulator driven by a synthesizer around 15 MHz, which corresponds to $\Delta\nu$ with a modulation index of 2.1. One sideband frequency of $\nu_L+\Delta\nu$ was used as the σ^+-polarized beam and the other of $\nu_L-\Delta\nu$ was used as the σ^--polarized beam. The fractional power of one sideband was 30% of the incident beam. Before the laser beam incident into the interaction region, we used a beam splitter for a single laser beam to divide into two parallel copropagating beams with equal intensities. A linear polarized laser beam was incident here. The beam spacing D was 8.1 mm or 24.4 mm. The magnetic field produced by a Helmholtz coil was applied perpendicular to the atomic beam and parallel to the laser beam. The fluctuation of the magnetic field in the region of the interferometer was about 0.1%. A half-wave plate was inserted in the path of the first beam before the interaction with the atomic beam, in order to give a variable optical phase difference between $\phi_1^{\sigma+}$ and $\phi_1^{\sigma-}$ by rotating the half-wave plate. The population of the upper state after the interactions were measured by monitoring the fluorescence with a photomultiplier from the $^3P_1$ state, approximately 300 mm downstream from the excitation region.

Figure 3 shows typical Ramsey fringes at a beam spacing D of 8.1 mm at a total laser power per interaction of 0.6 mW, which is about the pulse area of $\pi/2$ [17]. Around the resonance of $\Delta\nu-\Delta\nu_B$, a saturation dip appears with a depth of about 15% and a FWHM of about 400 kHz, which corresponds to the transit width. Near the center of the dip, the Ramsey fringes with a period of 50 kHz appear. As the detuning of $\Delta\nu-\Delta\nu_B$ increases, the interference fringe disappears gradually. This occurs due to the dispersion effect of the atomic beam.

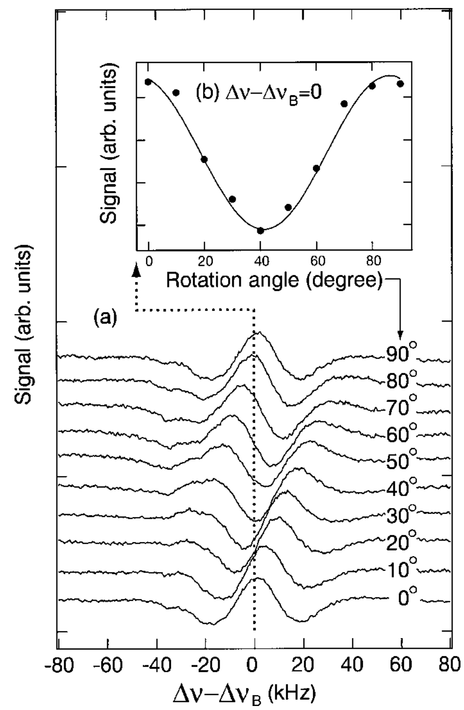

FIG. 4. (a) Ramsey fringes for various rotation angles of the half-wave plate. (b) The phase at the resonance of $\Delta\nu-\Delta\nu_B=0$ is shown as a function of the rotation angles of the half-wave plate, together with a sinusoidal curve.

Figure 4 shows the Ramsey fringes for various optical phase differences. The pattern of the Ramsey fringes varies on the relative optical phase. By rotating 45° the fringe reverses and the phase is shifted 2π at 90°. In Fig. 4(b) the amplitude of the fringe at $\Delta\nu-\Delta\nu_B=0$ is shown together with a sinusoidal curve. We can see a periodical fringe with a visibility of 6.5%. It should be noted that the fringe size does not decrease depending on the optical phase shift. Consequently, we can measure the nondispersive phase shift at the condition of $\Delta\nu-\Delta\nu_B=0$.

IV. MEASUREMENT OF THE AHARONOV-CASHER EFFECT

A. Experimental apparatus

The experimental apparatus for the measurement of the Aharonov-Casher effect is shown in Fig. 5. The calcium atomic polarizing white-color interferometer described in the preceding section was used. The two interaction zones were located in the electrode. The electrode was composed of a pair of stainless steel plates, which were 60 mm long, 20 mm wide, 5 mm thick, and spaced by 4.85 mm. This electrode was set so that the electric field was perpendicular to both the magnetic field and the atomic beam and produced the electric field of ± 25 kV/cm. The variation of the electric field in the entire interferometer region was about 1%.

The spacing of the two interaction zones was set at 24.4 mm, which produces the period of the Ramsey fringe of 16 kHz in order to get high resolution. However, the visibility of the interference signal decreased to 2.2%, which is about one

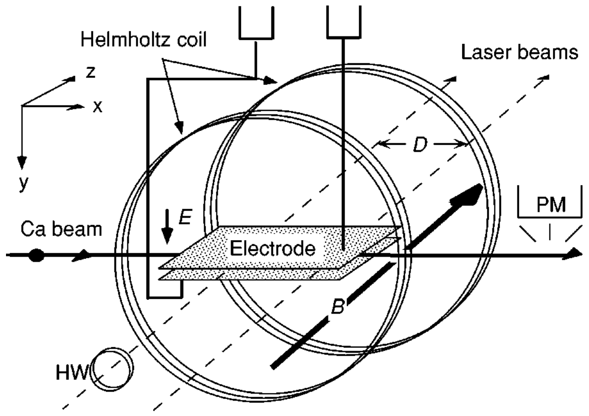

FIG. 5. Experimental setup for measurement of the Aharonov-Casher phase. Two laser beams compose the atomic polarizing white-color interferometer by irradiating the atomic beam in the center part of the electrode. Two stainless steel plates generate an electric field in the y axis, and a Helmhotz coil generates a magnetic field in the z axis. HW, half wave plate; PM, photomultiplier.

third of that at $D=8.1$ mm. So, the derivative signal of fringes was measured using a lock-in amplifier at an integration time of 1 s, with a modulation frequency of 30 Hz, and a modulation amplitude of 4 kHz. The typical derivative signal of Ramsey fringes is shown in Fig. 6. The signal-to-noise ratio was about 50.

B. Measurement of the Aharonov-Casher phase

Figure 7 shows a typical example of the measurement of the AC phase shift at an applied electric field of 11.1 kV/cm. According to Eq. (8), the resonance condition of $\nu_L \pm \Delta\nu$ is shifted by a small amount that is proportional to the fourth power of the electric field, in addition to the quadratic Stark shift. The largest visibility is obtained at a resonance condition, otherwise the visibility decreases due to the dispersion effect. In order to know the resonance frequency, at first we measured the two Ramsey resonances for a positive electric field and a negative electric field, and then set up the rf frequency in the middle of two resonance frequencies. Next, we measured the maximum and the minimum height of the interference fringes by rotating the half-wave plate. The difference between the maximum and the minimum height is equivalent to the phase difference of π. The phase was set at the middle position by regulating the half-wave plate. Then, we measured the phases for the electric fields of $+11.1$ kV/cm and -11.1 kV/cm via 0 kV/cm for 20 s by turns. The signal-to-noise ratio was about 60. The AC phase shift and the shift due to the resonance frequency under the electric-field were clearly observed. From the difference between the phases for $+11.1$ kV/cm and -11.1 kV/cm, the AC phase for an electric field difference of 22.2 kV/cm was obtained to be 153 ± 3 mrad.

The above process was repeated for several strengths of the electric field. Figure 8 shows the measured AC phase

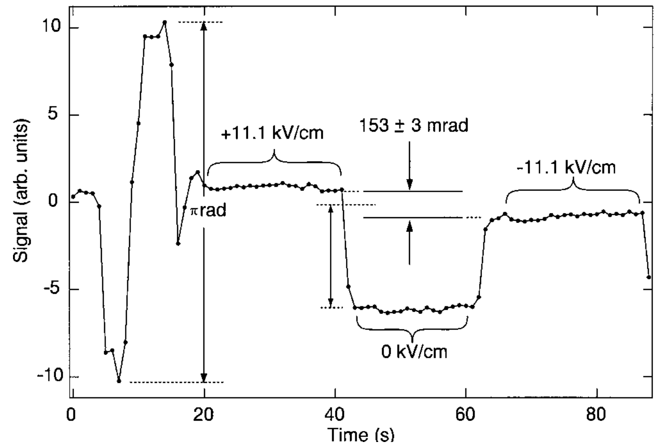

FIG. 7. Typical experimental result of the Aharonov-Casher phase at electric fields of ± 11.1 kV/cm. The rf frequency $\Delta\nu$ is shifted by $+1920$ Hz to compensate the tensor Stark effect on $m=\pm 1$. The fringe size was measured first and the phases for $+11.1$ kV/cm, 0 kV/cm, and -11.1 kV/cm were measured by turns. The difference between the phases for ± 11.1 kV/cm is the real AC phase. The phase for 0 kV/cm shifts from others due to the tensor Stark effect on $m=\pm 1$.

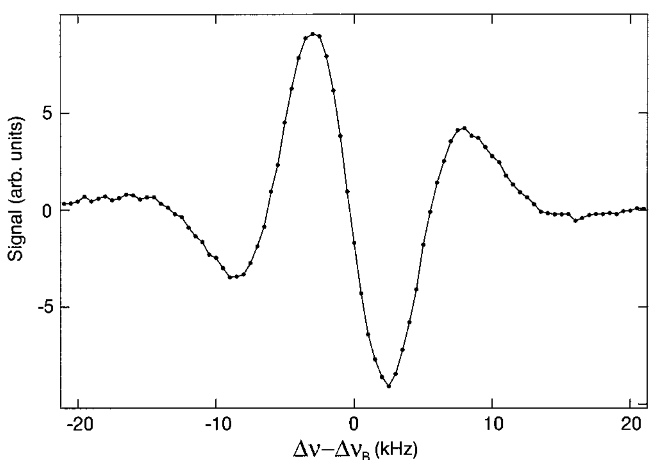

FIG. 6. Derivative Ramsey fringes as a function of $\Delta\nu-\Delta\nu_B$. Signals are detected at an integration time of 1 s every 500 Hz. The spacing of laser beams is 24.4 mm.

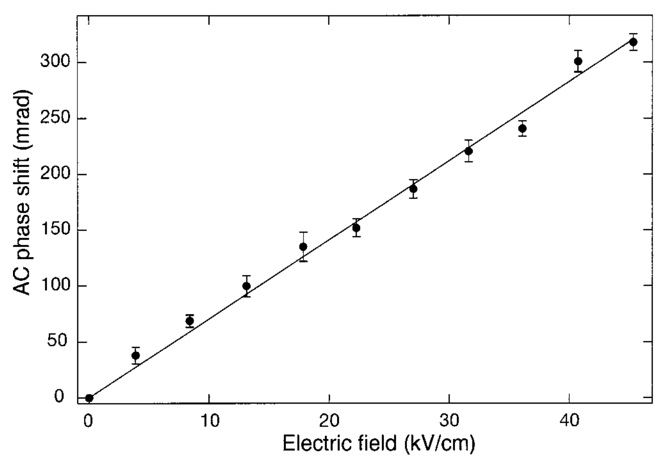

FIG. 8. Aharonov-Casher phase shift vs electric field strength. The experimental points are in good agreement with the theoretical prediction (solid line).

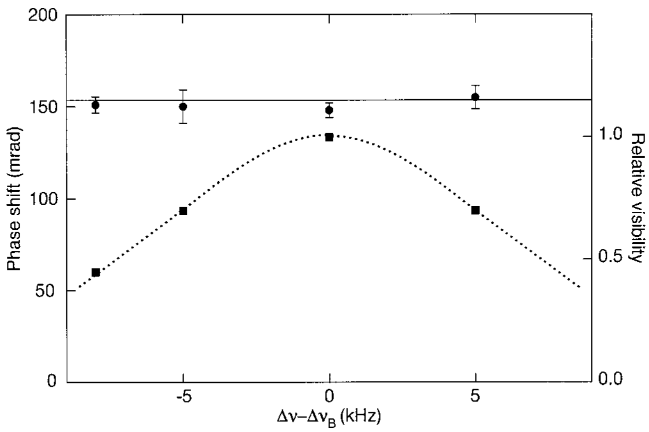

FIG. 9. Aharonov-Casher phase (circle) and the visibility of the interference fringes (square) vs the detuning of $\Delta\nu-\Delta\nu_B$. The visibility is normalized to the value of $\Delta\nu-\Delta\nu_B=0$.

shift as a function of the strength of electric field. A straight line was fitted by the least-squares fit to the data. In our experiment, the value of the slope has been determined to be 7.07 ± 0.18 kV/cm. The combined uncertainty was comprised of the statistical uncertainty of 2.5%, the uncertainty in the measurement of beam spacing of 0.2% and the uncertainty of the electric field of 1.4%, including systematic error from the electric-voltage source. Therefore, the ratio of the experimental result to the theory is

$$\frac{\Delta\psi_{\text{expt}}}{\Delta\psi_{\text{theor}}}=0.985\pm0.029. \tag{10}$$

We could confirm the theory of the Aharonov-Casher effect from a direct measurement of the phase without the use of the velocity of an atom. The present uncertainty obtained for such short measurement time could not be smaller than the previous results, but there will still be room for improvement by increasing the measurement time.

C. Dependence of AC phase shift on detuning of the rf frequency

In the preceding section, we measured the AC phase on the resonance condition. In contrast, Fig. 9 shows the AC phase shift vs a detuning of $\Delta\nu-\Delta\nu_B$ at an electric-field difference of 22.2 kV/cm, together with the relative fringe size. The results show that the phase shifts were independent of the detuning of $\Delta\nu-\Delta\nu_B$, while the fringe size decreases as the detuning increases. The decrease of the fringe size occurs due to the dispersion effect of the Ramsey phase. On the other hand, the fact that the AC phase does not depend on the rf detuning will be consistent that the AC phase is a nondispersive phase.

The verification of the nondispersive feature of the AC phase shift is very important, therefore, several authors investigated it by focusing their attention to the particle velocity, for example, by changing the velocity of the particle, or by using the velocity-selected particle. We also examined it at two different velocities of 810 m/s and 650 m/s, by changing the temperature of oven and the excitation power of the laser. Both results were in agreement within the error.

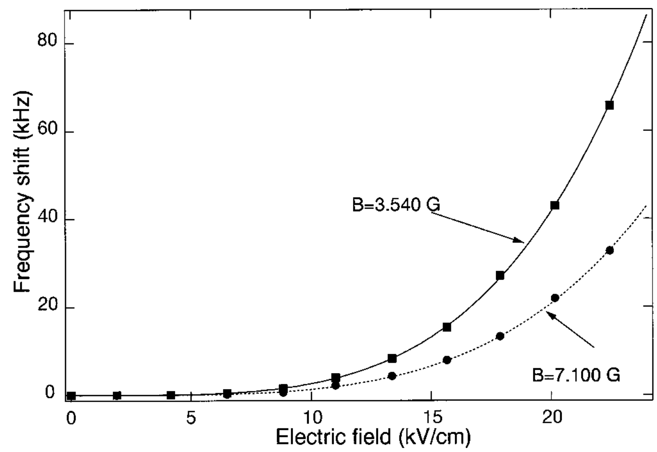

FIG. 10. Frequency shift due to the tensor Stark effect on the $m=\pm1$ state vs applied electric field. Circles and dotted line show measured values and a fitted curve at a magnetic fied of 7.10 G. Squares and solid line show measured values and a fitted curve, respectively, at a magnetic field of 3.54 G.

D. Tensor polarizability α_2 of the $^3P_1$ state

When the electric field is applied perpendicular to the magnetic field, the tensor stark effect splits the energies between the $m=+1$ and $m=-1$ state, depending on the strength of the electric field, according to Eq. (8), in addition to the Zeeman split. The effect was observed as a frequency shift of the Ramsey resonance or a phase shift, as shown in Fig. 7. Therefore, the tensor polarizability of the $^3P_1$ state in Ca was measured from the Ramsey resonance frequency. The mean values of the two Ramsey resonance frequencies for a positive and a negative electric field were plotted in Fig. 10, as a function of an electric field for two strengths of a magnetic field. We find that the frequency splitting is proportional to the fourth power of the electric field and inversely proportional to the magnetic field, although there are two values. This behavior is in good agreement with the Eq. (8).

The tensor polarizability α_2 was deduced to be $\alpha_2=2.623\pm0.015$ kHz/(kV/cm)^2. The present value was determined with higher accuracy, compared with the previous values of 3.2 ± 0.8 kHz/(kV/cm)^2 [18] and 3.0 ± 0.2 kHz/(kV/cm)^2 [19]. From the present value and the discussion of Ref. [18], the oscillator strength from ^3P to ^3D was deduced to be 0.068, which is close to 0.073 obtained by the semiempirical Hartree-Fock calculation [20].

V. CONCLUSION

We have developed an atomic polarizing white-color interferometer, which compared the partial waves of the $m=+1$ and $m=-1$ states, that were excited from the ground level with two resonance frequencies at two zones separated in space. The interferometer has properties that it generates on the Ramsey fringes as a detuning of the rf frequency from the difference between two resonance frequencies, while it produces white-color fringes as a detuning of the laser frequency.

We used this interferometer to measure the Aharonov-Casher phase directly in a comparatively short time by removing the Stark phase shift. The Aharonov-Casher phase that was proportional to the electric field was measured with the uncertainty of 2.5% for 20 s. The direct phase measurement verified the theoretical predictions with an uncertainty of 2.9%, as well as the previous measurements. From the frequency splitting between $m=+1$ and $m=-1$ states, the tensor polarizability of calcium ${}^3P_1$ state was determined to be $\alpha_2 = 2.623 \pm 0.015$ kHz/(kV/cm)^2.

We conclude that we could cancel out the dc Stark phase using the property of the polarizing interferometer. We could also cancel out the Zeeman shift using the property of the Ramsey resonance and we could measure the AC phase directly using the property of the white-color interferometer. The present excitation method will make possible to develope the atom interferometer composed of two long-lived excited states separated in the rf frequency. It will expand considerably the capability of atom interferometers for precise measuremenst or verifications of the fundamental physics.

ACKNOWLEDGMENTS

The authors acknowledge Dr. J. Helmcke and Dr. F. Riehle of PTB for their valuable discussions and support. In particular, A.M. acknowledges Dr. J. Helmcke for his suggestion that the white-color interferometer is suited for measurement of the Aharonov-Casher phase. The authors also give thanks to Dr. T. Kurosu of AIST/Japan for his discussions about the atom interferometer and Professor Y. Takahashi of University of Kyoto for his valuable comment on the tensor Stark effect. This research was partly supported by a Grant-in-Aid for Scientific Research on Priority Area (B) organized by Professor F. Shimizu, research of the Ministry of Education, Science, Sports, and Culture (Japan).

[1] Y. Aharonov and A. Casher, Phys. Rev. Lett. **53**, 319 (1984).
[2] Y. Aharonov and D. Bohm, Phys. Rev. **115**, 485 (1959).
[3] A. Cimmino, G. I. Opat, A. G. Klein, H. Kaiser, S. A. Werner, M. Arif, and R. Clothier, Phys. Rev. Lett. **63**, 380 (1989).
[4] K. Sangster, E. A. Hinds, S. M. Barnett, and E. Riis, Phys. Rev. Lett. **71**, 3641 (1993).
[5] K. Sangster, E. A. Hinds, S. M. Barnett, E. Riis, and A. G. Sinclair, Phys. Rev. A **51**, 1776 (1995).
[6] A. Görlitz, B. Schuh, and A. Weis, Phys. Rev. A **51**, R4305 (1995).
[7] K. Zeiske, G. Zinner, F. Riehle, and J. Helmcke, Appl. Phys. B: Lasers Opt. **60**, 205 (1995).
[8] A. Morinaga and Y. Ohuchi, Phys. Rev. A **51**, R1746 (1995).
[9] S. Yanagimachi, Y. Omi, and A. Morinaga, Phys. Rev. A **57**, 3830 (1998).
[10] Ch. J. Bordé, Phys. Lett. A **140**, 10 (1989).
[11] A. Morinaga, M. Nakamura, T. Kurosu, and N. Ito, Phys. Rev. A **54**, R21 (1996).
[12] S. Yanagimachi, K. Mizobuchi, and A. Morinaga, Phys. Rev. A **64**, 041601 (2001).
[13] A. Khadjavi, A. Livio, and W. Happer, Phys. Rev. **167**, 128 (1969).
[14] R. Druzdowski, J. Kwela, and M. Walkiewicz, Z. Phys. D: At., Mol. Clusters **27**, 321 (1993).
[15] M. Kasevich and S. Chu, Phys. Rev. Lett. **67**, 181 (1991).
[16] A. Morinaga, S. Yanagimachi, and T. Aoki, in *6th Symposium on Frequency Standards and Metrology, 2001*, edited by P. Gill (World Scientific, London, in press).
[17] F. Riehle, A. Morinaga, J. Ishikawa, T. Kurosu, and N. Ito, Jpn. J. Appl. Phys., Part 2 **31**, L1542 (1992).
[18] G. v. Oppen, Z. Phys. **232**, 473 (1970).
[19] K. Zeiske, PTB Report No. PTB-Opt-48, 1995 (unpublished).
[20] P. F. Grudzev, Opt. Spectrosc. **22**, 89 (1967).